Shielding of the A1 Domain by the D'D3 Domains of von Willebrand Factor Modulates Its Interaction with Platelet Glycoprotein Ib-IX-V*

Hans Ulrichts[‡1,2], **Miklós Udvardy**[‡§1], **Peter J. Lenting**[¶], **Inge Pareyn**[‡], **Nele Vandeputte**[‡], **Karen Vanhoorelbeke**[‡2], **and Hans Deckmyn**[‡3]

From the ‡Laboratory for Thrombosis Research, Interdisciplinary Research Center, Katholieke Universiteit Leuven Campus Kortrijk, B-8500 Kortrijk, Belgium, §Department of Clinical Biochemistry and Molecular Pathology, University Debrecen, Faculty of Medicine, H-4012 Debrecen, Hungary, and ¶Laboratory for Thrombosis and Haemostasis, Department of Haematology, University Medical Center Utrecht, 3584 CX Utrecht, The Netherlands

Soluble von Willebrand factor (VWF) has a low affinity for platelet glycoprotein (GP) Ibα and needs immobilization and/or high shear stress to enable binding of its A1 domain to the receptor. The previously described anti-VWF monoclonal antibody 1C1E7 enhances VWF/GPIbα binding and recognizes an epitope in the amino acids 764–1035 region in the N-terminal D'D3 domains. In this study we demonstrated that the D'D3 region negatively modulates the VWF/GPIb-IX-V interaction; (i) deletion of the D'D3 region in VWF augmented binding to GPIbα, suggesting an inhibitory role for this region, (ii) the isolated D'D3 region inhibited the GPIbα interaction of a VWF deletion mutant lacking this region, indicating that intramolecular interactions limit the accessibility of the A1 domain, (iii) using a panel of anti-VWF monoclonal antibodies, we next showed that the D'D3 region is in close proximity with the A1 domain in soluble VWF but not when VWF was immobilized; (iv) destroying the epitope of 1C1E7 resulted in a mutant VWF with an increased affinity for GPIbα. Our results support a model of domain translocation in VWF that allows interaction with GPIbα. The suggested shielding interaction of the A1 domain by the D'D3 region then becomes disrupted by VWF immobilization.

The plasma protein von Willebrand factor (VWF)[4] has a central role in normal primary hemostasis (1). The interaction of VWF with its platelet receptor glycoprotein (GP) Ibα in the GPIb-IX-V complex mediates platelet adhesion to extracellular matrices exposed at sites of vascular injury. This interaction is essential for thrombus formation at sites of high shear stress, as in microarterioles or in stenosed arteries.

Mature VWF comprises a series of multimers that are composed of homodimers interlinked through disulfide bridges. The mature VWF subunit consists of four distinct types of internal homology present in two to three copies in the following order from the N terminus: D'-D3-A1-A2-A3-D4-B1-B2-B3-C1-C2-CK.

Native VWF in solution has an extremely low affinity for GPIbα, suggesting the existence of specific regulatory mechanisms that maintain ligand and receptor in the same environment without adverse consequences. The affinity of VWF toward its primary receptor can be increased by artificial means, such as removal of sialic acid side chains (2) or the presence of modulators like the bacterial glycopeptide ristocetin (3) or the snake venom protein botrocetin (4). In pathophysiological conditions, however, binding is induced by immobilization of VWF or by elevated fluid shear stress, which is likely due to changes in interdomain interactions (5).

The VWF A1 domain (amino acids (aa) 1260–1479) contains the only known GPIbα binding site (6). A 39/34-kDa dispase fragment of human VWF (aa 1243/1244–1481) (7) and the recombinant VWF fragment VCL (aa 1267–1491) (8), both spanning the A1 domain, bind to platelet GPIb-IX-V in the absence of modulators, in contrast to full-length VWF. Therefore, it is not unlikely to suppose that the remainder of VWF, outside the A1 domain, serves as a masking environment, preventing binding to GPIb-IX-V. Conformational changes in VWF upon immobilization or upon exposure to shear might relieve this possible shielding effect of neighboring domains in VWF and might thereby reveal the functional binding site in the A1 domain. This mode of action is supported by kinetic and crystal studies, which demonstrated a higher binding affinity of the isolated A1 domain for GPIb-IX-V compared with full-length VWF (9–11). Moreover, these crystal studies confirm that conformational changes in both GPIbα and in the A1 domain are required for their mutual interaction.

The A1 domain contains a typical α/β-fold that is delimited by a single disulfide bridge (aa 1272–1456) (12). The N-terminal region in the A1 domain (aa 1260–1271), flanking the disulfide bridge, modulates the A1/GPIbα interaction; (i) crystal studies reveal a displacement of this flanking region upon binding to GPIbα (10, 11); (ii) naturally occurring mutations in this region have been reported to induce von Willebrand disease (VWD) type 2B phenotype, characterized by an increased affinity of VWF for GPIbα (13); (iii) Ala substitution mutants in this region show an increased affinity for GPIbα (14).

As mentioned before, it is suggested that neighboring domains in VWF might impede the accessibility of the GPIbα binding region. We have previously described a monoclonal antibody (moAb), 1C1E7, directed against the aa 764–1035 region in the N-terminal D'D3 domains of VWF (15). Although this moAb interacts with a region distinct from the VWF A1 domain, it induces von Willebrand disease-type 2B-like alterations (16). This would suggest that the binding region

---

FIGURE 1. **Schematic representation of a mature VWF subunit and the VWF deletion mutants used in this study.** Binding regions of the anti-VWF moAbs are indicated.
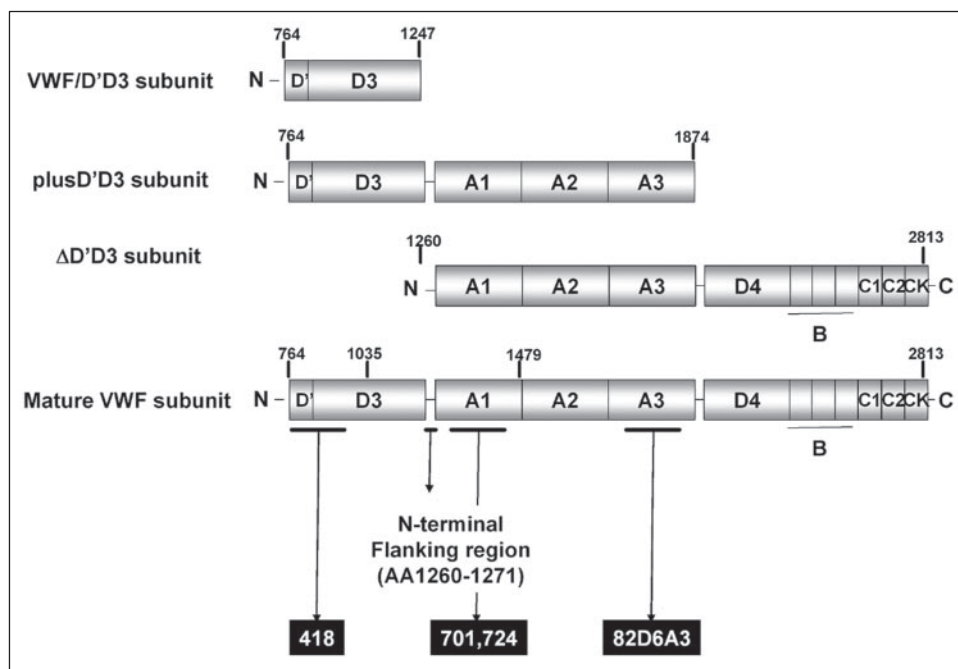
of 1C1E7 in VWF might have a modulatory role for the VWF/GPIbα interaction and could be a shielding region for the GPIbα binding domain. The objectives of this study were to obtain evidence for the functionality of the D'D3 region in VWF for GPIbα binding using deletion mutants, constructed VWF chimeras, and recombinant 1C1E7 as tools.

EXPERIMENTAL PROCEDURES

Materials—Different moAbs against VWF were described previously. moAb 82D6A3 binds to the VWF A3 domain and inhibits VWF binding to collagen types I, III, and IV (17), and moAb 1C1E7 recognizes the N-terminal part of VWF (aa 764–1035) (15). moAbs 724, 701, and 418 were kind gifts of Dr. J. P. Girma (INSERM U143, le Kremlin-Bicê-tre, Paris, France). moAbs 724 and 701 recognize the VWF A1 domain (18, 19), whereas moAb 418 interacts with the first 106 aa in mature VWF (20). VWF was purchased from the Red Cross (Brussels, Belgium). moAbs or VWF were biotinylated using EZ-link Sulfo-NHS-SS-Biotin (Perbio, Helsingberg, Sweden).

Pooled plasma was prepared from the plasma of 25 healthy volunteers (21). The vector pSV2-dhfr (22) was obtained from American Type Cell Culture (Manassas, VA). Restriction endonucleases were from MBI Fermentas (Vilnius, Lithuania).

Numbering of the aa sequence of VWF or the nucleotide sequence of the VWF gene starts with, respectively, the initiator methionine or the start codon as the +1 position. Recombinant VWF/D'A3 (aa 1–1874), VWF/D'D3 (aa 1–1247), and VWF/A1-CK (1260–2813) were expressed and purified as described before (23). For clarity, we renamed VWF/D'A3 and VWF/A1-CK as plusD'D3 and ΔD'D3, respectively. A representation of VWF, its fragments, and the binding sites of the moAbs is shown in Fig. 1.

Construction and Expression of 1C1E7 Single-chain Variable Fragment—Total cell RNA was extracted from 1C1E7-expressing hybridoma cells using the RNeasy mini kit (Qiagen, Venlo, The Netherlands) and was reverse-transcribed in the ThermoScript reverse transcription-PCR system (Invitrogen) using oligo(dT)$_{20}$ primers.

The N-terminal sequence of the heavy and light chain of 1C1E7 was determined by TopLab (Martinsried, Germany). Based on these data,

degenerate sense primers were designed for the heavy and the light chain variable regions (V_H and V_L, respectively), and framework-specific antisense primers were used in the subsequent PCR reactions (24, 25). Amplification of V_H was performed using *Pfu* Turbo DNA polymerase (Stratagene, La Jolla, CA), and the resulting PCR product was ligated in the pCR®-Blunt vector (Invitrogen). V_L was amplified with Platinum® *Taq* DNA polymerase (Invitrogen), and the resulting PCR product was ligated in the pCR®2.1-TOPO® vector (Invitrogen). For the construction of the 1C1E7 single-chain variable fragment (scFv), both V_H and V_L were extended such that the following splice overlapping extension PCR resulted in a V_H-$(G_4S)_3$-V_L scFv coding sequence. This PCR product was ligated in the pSecTag/FRT/V5-His vector (Invitrogen).

The 1C1E7 scFv was expressed in *Escherichia coli* as a His-tag fusion protein. Briefly, NcoI and XhoI restriction sites were added to the 3′ and 5′ ends, respectively, by PCR using sequence-specific primers. The 1C1E7 scFv DNA was cloned in the pET26+ vector (Stratagene) using the NcoI and XhoI restriction sites. BL-21 *E. coli* were transformed with the construct and were induced for 2 h with 0.5 M isopropyl-β-D-galactoside. The bacteria were harvested (10,000 × *g* for 10 min), and cell proteins from the pellet were extracted with the BugBuster protein extraction reagent (Novagen, Merck). 1C1E7 scFv was expressed as inclusion bodies. To refold the scFv, inclusion bodies were dissolved in IB buffer (6 M guanidine-HCl, 1.5 M urea, 0.6 mM reduced glutathione, 0.3 mM oxidized glutathione in phosphate-buffered saline, PBS) (26). The solubilized proteins were subsequently dialyzed against a series of urea solutions (8, 6, 4, and 2 M overnight (ON) at 4 °C) and, finally, against PBS.

Ristocetin- and Botrocetin-induced Binding of VWF, ΔD'D3, plusD'D3, or Recombinant VWF to a Recombinant GPIbα Fragment (aa 1–289)—The ristocetin- and botrocetin-induced binding of VWF, ΔD'D3, plusD'D3, or recombinant VWF (see later) to a GPIbα fragment was performed as previously described (21). Briefly, microtiter plates were coated ON at 4 °C with anti-GPIbα moAb 2D4 (5 μg/ml in PBS) and blocked with Tris-buffered Saline (TBS) containing 3% milk powder. A recombinant N-terminal, VWF binding GPIbα fragment (aa 1–289) (rGPIbα) was expressed in Chinese hamster ovary cells and

purified as described (27). Wells were incubated for 1.5 h at 37 °C with rGPIbα (1 μg/ml in TBS, 0.1% Tween 20) and incubated for 1.5 h at 37 °C with a dilution series of ristocetin (abp, New York, NY) or botrocetin purified from crude *Bothrops jararaca* venom (Sigma) (28) in the presence of a constant amount of purified VWF, ΔD'D3, plusD'D3, or recombinant VWF (0.5 μg/ml) and in the absence or presence of 12 μg/ml 1C1E7 IgG. Bound VWF, ΔD'D3, plusD'D3, or recombinant VWF was detected for 45 min at room temperature (RT) with a 1/3000 dilution of anti-VWF polyclonal antibodies labeled with horseradish peroxidase (anti-VWF-Ig-horseradish peroxidase, Dako, Glostrup, Denmark). Visualization was obtained with H_2O_2 and *ortho*-phenylenediamine (Sigma), and the coloring reaction was stopped with 4 M H_2SO_4, after which the absorbance was determined at 490 nm.

Platelet Agglutination—Agglutination studies were performed in an Elvi-840 dual channel aggregometer (Pabish, Brussels, Belgium) with constant stirring at 1000 rpm at 37 °C.

For the agglutination experiments using 1C1E7 scFv, blood was drawn from healthy volunteers on trisodium citrate, pH 7.5 (0.11 M, 10:1 v/v), and centrifuged at 180 × *g* for 10 min to obtain platelet-rich plasma. Platelet-rich plasma was incubated for 3 min with buffer and with 1C1E7 scFv or IgG, after which agglutination was induced by the addition of ristocetin.

For the agglutination experiments using the VWF fragments, blood was collected on acid citrate dextrose (0.085 M trisodium citrate, 0.065 M citric acid, 0.110 M glucose, pH 4.5) (10:1.5 v/v). Platelets were washed twice and resuspended in PBS containing 1 mg/ml glucose and 1 mg/ml bovine serum albumin. A final platelet concentration of 200,000 platelets/μl was used. ΔD'D3, plusD'D3, or VWF/D'D3 were added to a final concentration of 10 μg/ml, and the mixture was incubated for 3 min, after which agglutination was induced by the addition of ristocetin.

Construction of Expression Plasmid for Chimeric Porcine/Human Recombinant VWF—An expression plasmid for a chimeric porcine/human recombinant VWF in which the aa 786–960 region of the human sequence was exchanged by the corresponding porcine sequence was constructed. This recombinant VWF construct is further referred to as VWF(aa786–960)PIG.

Briefly, the expression vector pNUT-VWF cas (29) was digested with the restriction endonuclease BglII, and the resulting 4.7-kilobase fragment was ligated subsequently in the unique BglII site of the vector pSV2-dhfr to give the vector pSV2-pNUT.

RNA was isolated from a porcine umbilical cord using the mRNA isolation kit (Roche Molecular Biochemicals), and cDNA was prepared with the Thermoscript™ reverse transcription-PCR system (Invitrogen) using the sequence specific primer RP3 (5′-CGC AGG TTC CTC TCC TCG CAG TTC-3′, nucleotides 3384–3408). cDNA was amplified by PCR using the sense primer P5 (5′-CGC AGC AAG AGG AGT CTG AGC TGC CGG CCC CCC ATG-3′, nucleotides 2279–2314) and the antisense primer RP3. The PCR product was ligated in the vector PCR4 Blunt-TOPO vector (Invitrogen). A unique EagI restriction site at position 2875 was introduced by PCR using the sense primer P5 and the point-mutated antisense primer P6.2 (5′-GAT GAA CCG GCC **G**GA TTC CAC3′, nucleotide 2867–2887). The PCR product was cloned in the pBAD-TOPO TA vector (Invitrogen) to give the vector pBAD-PIG.

Subsequently, the XhoI-EagI fragment of the vector pBAD-PIG was ligated in XhoI-EagI-digested pSV2-pNUT to give the vector pSV2-pNUT-PIG. The vector pSV2-pNUT-PIG was digested with EcoRI and BglII. The resulting 4.7-kilobase fragment was exchanged by the corresponding sequence of pNUT-VWF cas to give the final expression vector pNUT-VWF PIG.

Construction of Expression Plasmids for VWF Point or Double Mutants—Expression plasmids for human VWF or for VWF(aa786–960)PIG containing K968S, K991Q or S1009G,N1011S mutations were constructed starting from the plasmid pSV2-pNUT or pSV2-pNUT-PIG, respectively. Using the QuikChange XL site-directed mutagenesis kit (Stratagene) and specific primers, the desired mutations were introduced. The resulting vectors were digested with EcoRI and BglII, and the resulting 4.7-kilobase fragment was exchanged by the corresponding sequence of pNUT-VWF cas or pNUT-VWF PIG as described above to obtain expression plasmids for full-length VWF.

Expression of Recombinant VWF—VWF was transiently expressed in COS-7 cells (30) or stably expressed in baby hamster kidney cells overexpressing furin (BHK-fur) as described before (6). The VWF:Ag level was determined in a sandwich immunoassay as previously described (21).

Binding of VWF to moAb 1C1E7—96-Well microtiter plates (Greiner, Frickenhausen, Germany) were coated ON at 4 °C with moAb 1C1E7 (10 μg/ml in PBS), blocked for 2 h at RT with TBS containing 3% milk powder, and incubated for 2 h at 37 °C with a dilution series of VWF expression medium in TBS containing 0.3% milk powder. Bound VWF was detected as described above.

Binding of VWF to Human Collagen Type III—96-Well microtiter plates were coated ON at 4 °C with 25 μg/ml human collagen type III (Sigma) in PBS. Wells were blocked with PBS containing 3% milk powder and incubated with a dilution series of purified recombinant VWF in PBS containing 0.3% milk powder. Bound VWF was detected as described above (24).

Multimeric Analysis—The multimeric pattern of VWF was determined essentially as described (31). Briefly, 0.08 μg of VWF was separated on SDS 0.65% Seakem HGT, agarose gel (Cambrex, Bio Science Rockland, Inc., ME). Gels were fixed on Gelbond (Cambrex), and VWF was immunodetected using anti-VWF-Ig labeled with alkaline phosphatase (32) and further revelation with the AP conjugate substrate kit (Bio-Rad).

Cross-blocking Analysis for Antibody Binding to Immobilized VWF—96-Well microtiter plates were coated ON at 4 °C with VWF (10 μg/ml in PBS) and blocked for 2 h at RT with TBS containing 3% milk powder. Wells were incubated for 1 h at 37 °C with biotinylated moAb 418 (b-418) at its half-maximal binding concentration (0.15 μg/ml) in the presence of the competing moAbs 701, 724, 418, or 82D6A3 (15 μg/ml) using TBS containing 0.3% milk powder as buffer. Residual bound b-418 was detected for 45 min at RT with peroxidase-labeled streptavidin (1/10000 in TBS containing 0.3% milk powder). Visualization was performed as described above.

Cross-blocking Analysis for Antibody Binding to "Soluble" VWF—96-Well microtiter plates were coated with moAb 418 (2 μg/ml in PBS) and blocked for 2 h at RT with TBS containing 3% milk powder. Biotinylated VWF (b-VWF, 6 μg/ml) was preincubated with one of the anti-VWF moAbs (0.5–60 μg/ml) for 1 h at 37 °C after which this solution was transferred to the coated wells. After a further incubation of 30 min at 37 °C, residual bound b-VWF was detected with peroxidase-labeled streptavidin as described above.

Statistics—In this study means and S.E. are shown. Statistical significance of differences between means was evaluated using Student's *t* test.

RESULTS

Functionality of VWF Lacking the D'D3 Region—It has been suggested that the remainder of VWF outside the A1 domain might shield the GPIbα binding region. However, the exact mechanism of this

FIGURE 2. **Ristocetin- and botrocetin-induced binding of VWF(−fragments) to rGPIbα.** Microtiter plates were coated with anti-GPIbα moAb 2D4 and incubated with rGPIbα. Wells were incubated with a constant amount of ΔD'D3 (*filled bars*) or plusD'D3 (*open bars*) in the presence or absence of 1C1E7 IgG (12 μg/ml) and in the presence of ristocetin (*A*) or botrocetin (*B*) at the indicated amounts. Bound VWF was detected (mean ± S.E., *n* = 3). *NS*, not significant.
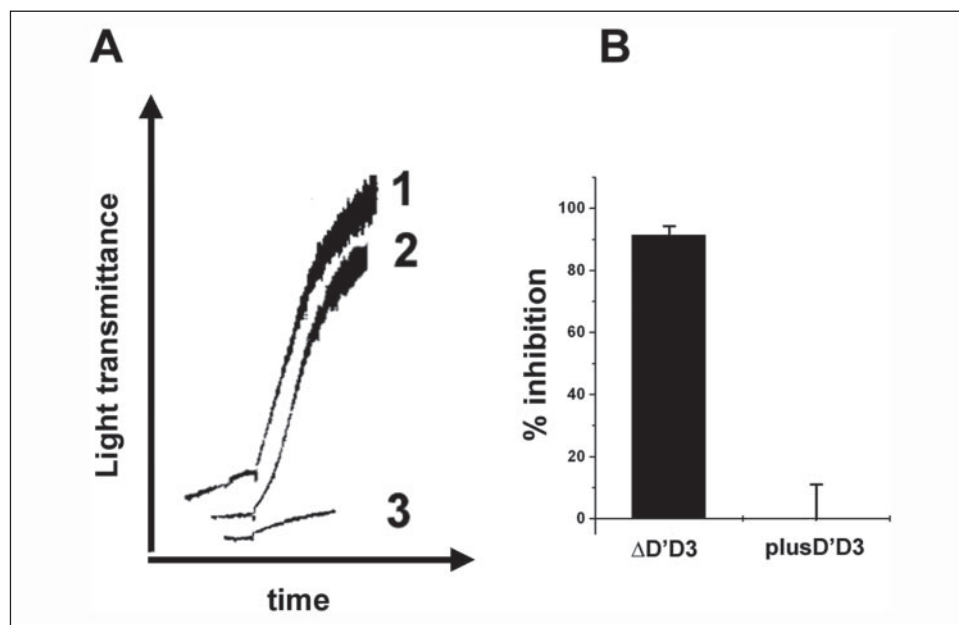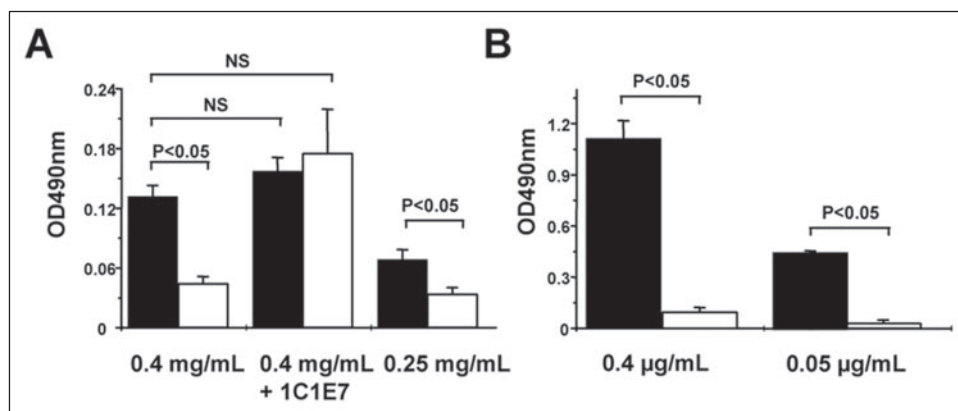

FIGURE 3. **Ristocetin-induced platelet agglutination.** *A*, washed platelets (200,000 platelets/μl) were incubated with 10 μg/ml ΔD'D3 (*1*) or plusD'D3 (*2* and*3*) after which agglutination was induced by the addition of 0.1 mg/ml ristocetin (*1* and *3*) or 0.2 mg/ml ristocetin (*2*). Results are representative of three independent experiments. *B*, washed platelets (200,000 platelets/μl) were incubated with 10 μg/ml ΔD'D3 or plusD'D3 in the presence of 10 μg/ml VWF/D'D3, after which agglutination was induced by the addition of a threshold dose of ristocetin (0.1 and 0.2 mg/ml, respectively). The percentage inhibition is shown (mean ± S.E., *n* = 3). As the 100% value, agglutination in the absence of VWF/D'D3 was chosen.

shielding has not been elucidated yet. The anti-VWF moAb 1C1E7 interacts with the aa 764–1035 region in the N-terminal D'D3 domains and modulates the binding of VWF to GPIbα. This would suggest a functional role of the D'D3 region in the binding of the A1 domain to its receptor. Therefore, we decided to study this putative modulatory role using VWF constructs lacking the D'D3 region.

Recombinant ΔD'D3 (aa 1260–1874) is a dimer composed of two VWF monomers lacking the D'D3 region but still contains the N-terminal flanking region of the VWF A1 domain. We verified the ristocetin- and botrocetin-induced binding of this construct to a recombinant GPIbα fragment and compared its affinity to that of recombinant plusD'D3 (aa 1–1874). This construct is a dimer as well but lacks the C-terminal D4-B1-B2-B3-C1-C2-CK regions.

In the presence of ristocetin as a modulator, ΔD'D3 interacted stronger with rGPIbα compared with plusD'D3 (Fig. 2*A*). Similar results were obtained with botrocetin (Fig. 2*B*). These results suggest that the D'D3 region has an inhibitory effect on the interaction of the A1 domain with GPIbα. The addition of 1C1E7 to plusD'D3 increased ristocetin-induced binding to rGPIbα to the level of ΔD'D3 while not affecting the GPIbα interaction of ΔD'D3 (Fig. 2*A*). This suggests that the observed effects are likely not due to a different affinity of the deletion mutants for the modulators used in the assay.

We further identified the inhibitory role exhibited by the D'D3 region in VWF/GPIbα interaction in platelet agglutination experiments.

Dimeric constructs were used because previous studies demonstrated the necessity of the use of at least dimeric molecules for sustaining platelet aggregation (33). The threshold dose needed for ristocetin-induced agglutination of washed platelets was lower for ΔD'D3 than for plusD'D3 (Fig. 3*A*), also demonstrating the inhibitory effect of the D'D3 region on the interaction of VWF with GPIbα.

In line with this, VWF/D'D3 inhibited the ristocetin-induced agglutination supported by ΔD'D3 while having no effect on the agglutination supported by plusD'D3 (Fig. 3*B*). These results show that the lack of inhibition by deletion of the D'D3 region in ΔD'D3 could be reverted by external addition of these isolated D'D3 domains.

These experiments demonstrate the functionality of the D'D3 region in the interaction of VWF with GPIbα, strongly suggesting that this region shields the GPIbα binding site in VWF, restricting its accessibility and preventing spontaneous VWF binding to platelets.

Epitope Mapping of moAb 1C1E7—To discover residues in the D'D3 region that would be responsible for its inhibitory effect, we identified the binding region of 1C1E7 in VWF. Previous studies demonstrated that 1C1E7 interacted with a tryptic fragment comprising the aa 764–1035 sequence in VWF, which is located in the D'D3 region (15). The location of the epitope was further corroborated by the fact that 1C1E7 failed to interact with ΔD'D3 but recognized the isolated D'D3 region (data not shown). Because 1C1E7 does interact with VWF in Western blot, this moAb probably recognizes a linear epitope. Therefore, the
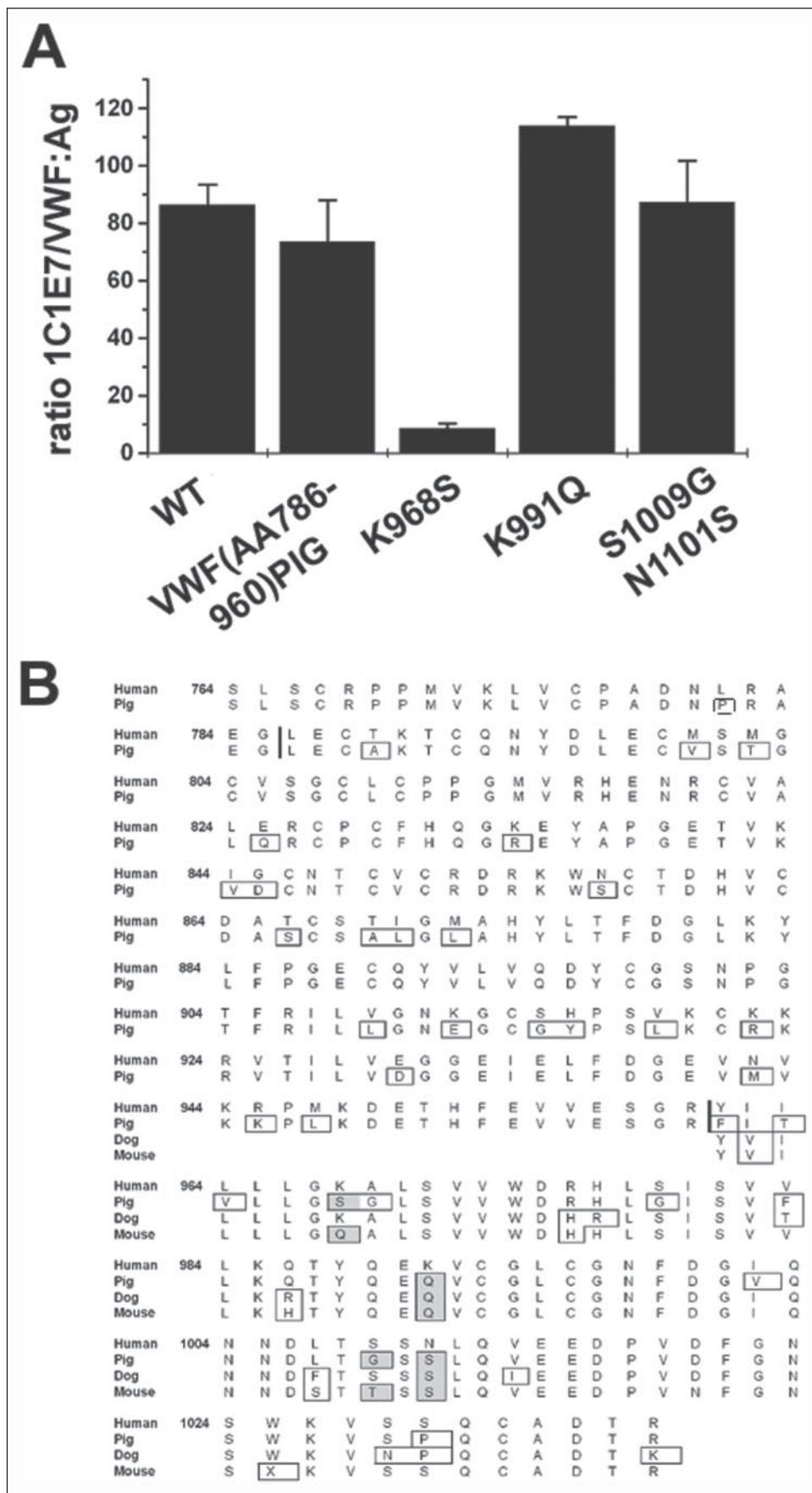
FIGURE 4. **Epitope mapping of 1C1E7.** *A*, binding of recombinant WT and mutant VWF to 1C1E7. Microtiter plates were coated with 1C1E7 or anti-VWF-Ig and incubated with expression medium of recombinant VWF. Bound VWF was detected with anti-VWF-Ig-horseradish peroxidase. The ratio of the A_{490} nm values for the 1C1E7 binding on the values for the anti-VWF-Ig are shown in percentages (mean $\pm$ S.E., $n = 3$). *B*, alignment of the primary sequence of human, canine, porcine, and murine VWF in the aa 764–1035 region. Sequence alignment of human (Medline submission number NP_000543), canine (Q28295), porcine (Q28833), and murine (NM_017708) VWF. The aa 786–961 fragment, which was exchanged in the chimeric construct, is delineated. Residues between aa 961–1035 that are different between human and porcine, canine, or murine VWF are *marked* with *boxes*. The residues that are different between human and both porcine and murine VWF but are similar between human and canine VWF are *shaded* in *gray*.
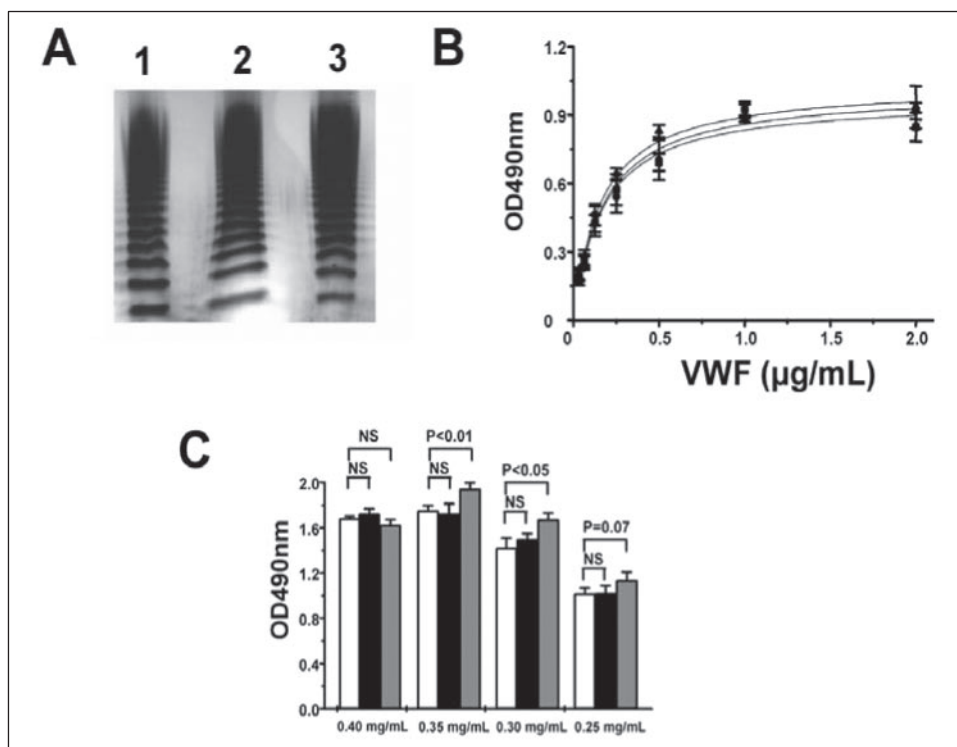
FIGURE 5. **Functionality of chimeric constructs.** *A*, VWF multimer analysis. Samples of WT VWF (*1*), VWF(aa786–960)PIG (*2*), and VWF(aa786–960)PIG-K968S (*3*) were analyzed by SDS-0.65% agarose gel electrophoresis and detected with anti-VWF-Ig labeled with alkaline phosphatase. *B*, collagen binding assay. Microtiter plates were coated with human collagen type III and incubated with a dilution series of WT VWF (■), VWF(aa786–960)PIG (●), and VWF(aa786–960)PIG-K968S (▲), after which bound VWF was detected (mean ± S.E., *n* = 3). *C*, ristocetin-induced binding of VWF to rGPIbα. Microtiter plates were coated with anti-GPIbα moAb 2D4 and incubated with rGPIbα. Wells were incubated with WT VWF (*open bars*), VWF(aa786–960)PIG (*filled bars*), and VWF(aa786–960)PIG-K968S (*gray bars*) (0.5 μg/ml) in the presence of ristocetin at the indicated amounts. Bound VWF was detected (mean ± S.E., *n* = 3). *NS*, not significant.

cross-reactivity of 1C1E7 with VWF of different species was verified to determine if differences in the primary structure of VWF have an effect on the binding of 1C1E7.

1C1E7 failed to recognize porcine plasma VWF but was still able to interact with canine VWF (data not shown). This suggests that some of the 35 residues in the aa 764–1035 region of human VWF that are not shared with the porcine VWF sequence might maintain the epitope of 1C1E7. To identify these residues, a chimeric recombinant VWF (VWF(aa786–960)PIG) in which the aa 786–960 region of the human sequence was exchanged by the corresponding porcine sequence was constructed. For cloning reasons, only this part of the N-terminal aa 764–1035 region in human VWF was exchanged. This construct, containing 23 residues differing from the human sequence, was transiently expressed in COS-7 cells, and the interaction with 1C1E7 was determined. 1C1E7 still interacted with VWF(aa786–960)PIG (Fig. 4*A*), suggesting that the aa 961–1035 region in VWF probably maintains the epitope of this moAb. Further comparison of the primary sequence of human VWF in this region with sequences of porcine, canine, and murine VWF highlighted residues Lys-968, Lys-991, Ser-1009, and Asn-1011 as possible candidates for maintaining the epitope of 1C1E7 (Fig. 4*B*). These residues are different between human and both porcine and murine VWF but are similar between the human and canine protein. VWF mutants in which these residues were exchanged for the porcine analogues were constructed and transiently expressed in COS-7 cells. 1C1E7 bound as strongly with the K991Q and S1009G, N1011S mutant as to WT VWF, suggesting that these residues are not important for maintaining the epitope. However, binding was completely abolished for the K968S point mutant, identifying this residue as critical for the interaction of 1C1E7 (Fig. 4*A*).

Functionality of Chimeric Recombinant VWF—In a next step the ristocetin-induced binding of the recombinant full-length WT VWF and chimeric constructs to GPIbα was measured to verify if altering the structure in the D′D3 region might influence this interaction. Recombinant WT VWF, VWF(aa786–960)PIG, and VWF(aa786–960)PIG, in which a K968S point mutation was inserted (VWF(aa786–960)PIG-K968S), were expressed in BHK-fur (baby hamster kidney cells overexpressing furin) cells. The multimeric pattern of both mutants was similar to WT VWF with at least 16 detectable multimer bands (Fig. 5*A*). Binding characteristics of the mutants to anti-VWF moAbs 418, 82D6A3, 701, and 724 was similar to WT VWF (data not shown), suggesting a similar overall structural fold.

Next, the functional effects of the exchange of several residues in the D′D3 region was verified. The interaction with fibrillar collagen was not statistically different for mutant VWF as compared with the WT, resulting in a VWF:collagen binding assay of 1.09 ± 0.06 and 1.10 ± 0.07 units/ml for VWF(aa786–960)PIG (*p* = 0.28, *n* = 3) and VWF(aa786–960)PIG-K968S (*p* = 0.25, *n* = 3), respectively, using WT VWF as a reference (Fig. 5*B*).

VWF(aa786–960)PIG and VWF(aa786–960)PIG-K968S bound comparably to rGPIbα in the presence of 0.4 mg/ml ristocetin (Fig. 5*C*). However, at submaximal doses of ristocetin, VWF(aa786–960)PIG-K968S showed a small but significant increase in binding compared with VWF(aa786–960)PIG and WT. These results suggest that altering residues in the D′D3 region and, more specifically the binding region of 1C1E7, influences the binding affinity of VWF for GPIbα.

Cross-blocking Studies—Next, the structural proximity of the D′D3 region with the A1 domain in immobilized VWF and in soluble VWF was verified by analyzing whether binding of moAb 418 (interacting with the D′D3 region) could be blocked by moAbs 701 and 724 (both interacting with the A1 domain). This would give us the opportunity to gather information on the structural changes in VWF upon immobilization. As a negative control, moAb 82D6A3 (interacting with the A3 domain) was used. Two different enzyme-linked immunosorbent assay set-ups were developed, (i) cross-blocking of binding of b-418 to immobilized VWF by unlabeled moAbs and (ii) the inhibition of the capture of b-VWF to immobilized moAb 418 by the unlabeled moAbs. Previous data demonstrated that biotinylation of VWF had no effect on the interaction with fibrillar collagen or GPIbα, which would suggest that the
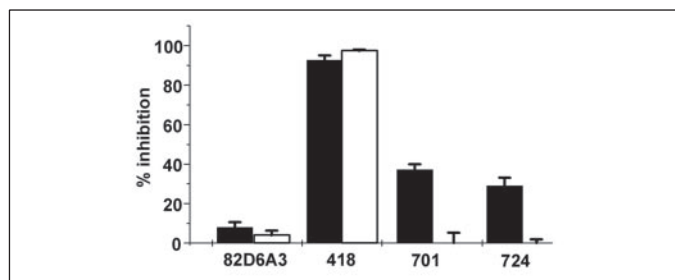
FIGURE 6. **Cross-blocking studies; inhibition of the binding of b-418 to immobilized VWF or b-VWF to immobilized moAb 418 by anti-VWF moAbs.** Microtiter plates were coated with VWF (*open bars*) or with moAb 418 (*filled bars*) and incubated with b-418 or b-VWF, respectively, in the presence of the anti-VWF moAbs 82D6A3, 418, 701, or 724. Residual bound b-418 or b-VWF was detected. Percentage inhibition is shown (mean ± S.E., $n = 3$). As a 100% reference, the binding of b-418 to immobilized VWF or the binding of b-VWF to immobilized 418 was chosen.

conformation of VWF is not altered upon biotinylation (34). When VWF was immobilized, no measurable inhibition of the binding of b-418 was observed by any of the moAbs except with unlabeled 418 as the positive control (Fig. 6, *open bars*), although all moAbs were able to interact with immobilized VWF (data not shown). In contrast, moAbs 701 and 724 did compete with moAb 418 for the binding to soluble b-VWF, whereas moAb 82D6A3 had again no effect (Fig. 6, *filled bars*).

This would suggest that in solution the A1 domain and the D′D3 region are in close proximity since moAbs interacting with these regions cross-block each other. However, when VWF was immobilized, moAbs interacting with the A1 domain failed to block binding of moAb 418 interacting with the D′D3 region, suggesting that these regions are now more distant from each other.

Construction and Expression of 1C1E7 scFv—To further characterize the VWF-activating potency of the moAb 1C1E7, the scFv was expressed as a His-tagged fusion protein in *E. coli*. 1C1E7 scFv increased ristocetin-induced platelet aggregation, similarly to 1C1E7 IgG (Fig. 7A), providing evidence that the construction was correct. Moreover, 1C1E7 scFv inhibited binding of the IgG to VWF, suggesting a same interaction site in VWF (data not shown). Comparison of the primary sequence of the complimentarity determining region 3 of the 1C1E7 heavy chain revealed a strong similarity with the N-terminal flanking region of the VWF A1 domain (Fig. 7B). As mentioned before, there is good evidence that this N-terminal flanking region modulates the binding of VWF to GPIbα. Based on our observation, we hypothesized that 1C1E7 might be able to mimic this region of the A1 domain. Because 1C1E7 does bind to the D′D3 region in VWF, the N-terminal flanking region of the A1 domain might have similar binding characteristics. This putative interaction of the A1 domain with the D′D3 region could modulate the VWF binding to GPIbα.

DISCUSSION

Human VWF in solution does not interact with its platelet receptor GPIb-IX-V under normal conditions. Binding, however, is induced by immobilization of VWF or by exposure to shear. These observations suggest that the affinity toward GPIb-IX-V is regulated by conformational changes in VWF that are induced by shear and/or immobilization and lead to exposure of functional sites.

In vitro, binding of VWF to GPIb-IX-V can be provided by modulators such as ristocetin or botrocetin. Although in these conditions binding is induced rather artificially, it has been demonstrated that ristocetin-dependent interactions quite closely correlate with the physiological shear-dependent situation (35).

We have previously identified the moAb 1C1E7 (15) which interacts with the aa 764–1035 region in the N-terminal D′D3 domains in VWF,
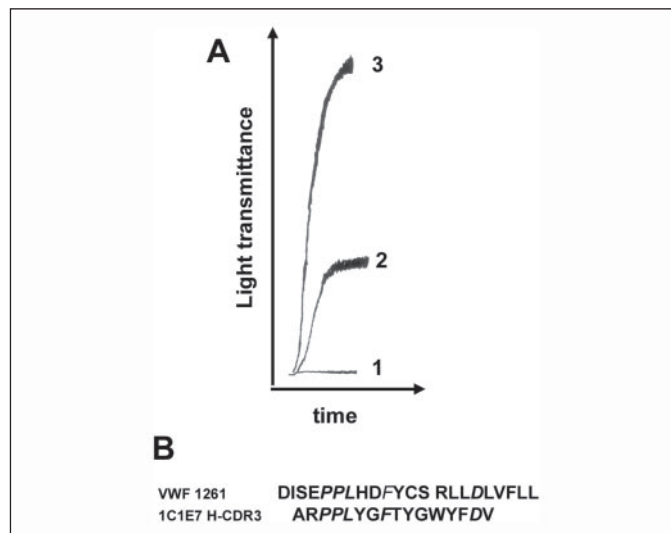

FIGURE 7. **Functionality of 1C1E7 scFv.** *A*, stimulating effect of 1C1E7 scFv on platelet aggregation in platelet-rich plasma. Platelet-rich plasma was incubated with PBS buffer (*1*), 1C1E7 scFv refolded from inclusion bodies (~20 µg/ml) (*2*), or 25 µg/ml 1C1E7 IgG (*3*), after which a subthreshold dose of ristocetin (0.2 mg/ml) was added. Results are representative of three independent experiments. *B*, alignment of the primary sequence of the N-terminal flanking region of the human A1 domain and the complimentarity determining region 3 of the 1C1E7 heavy chain.

increases the affinity of VWF for GPIbα, and hence, induces von Willebrand disease type 2B alterations, although it does not bind near the GPIb-IX-V binding site (16). This would suggest a modulatory effect for the binding region of 1C1E7 in VWF on the GPIbα interaction. Therefore, the goal of this study was to determine the functional role of the D′D3 region in binding of VWF to GPIb-IX-V.

Deletion of the D′D3 region in VWF resulted in a higher affinity for GPIbα as demonstrated in an enzyme-linked immunosorbent assay system; the dimeric deletion mutant ΔD′D3, lacking the D′D3 region, showed an increased ristocetin- and botrocetin-induced interaction with a recombinant GPIbα fragment compared with the dimeric deletion mutant plusD′D3, which lacks the C-terminal region in VWF. The addition of 1C1E7 IgG to plusD′D3 increased the ristocetin-induced binding to rGPIbα, now equaling the binding of ΔD′D3. This confirms again the modulatory effect of 1C1E7 on the VWF/GPIbα interaction but in addition proves that the observed difference in affinity of both deletion mutants for GPIbα is not due to a different affinity for ristocetin. These results were confirmed in a platelet agglutination assay; the threshold dose of ristocetin needed to induce agglutination of washed platelets was lower in the presence of ΔD′D3 as compared with plusD′D3. Moreover, at lower platelet concentrations, ΔD′D3 was able to sustain spontaneous platelet agglutination in contrast to plusD′D3 (data not shown). All together, these data strongly suggest that the D′D3 region may act as an inhibitory region, shielding the A1 domain in VWF.

Our data further confirm and extend previous studies that demonstrated the putative shielding of the GPIb binding site in the A1 domain by the N-terminal flanking regions of the A1 domain (aa 1260–1271) and the C-terminal region of the D3 region (aa 1204–1259). (i) Peptides derived from these regions inhibited ristocetin-induced binding of purified VWF to human platelets (36), (ii) stepwise N-terminal deletions in the aa 1204–1271 region of a recombinant VWF fragment comprising the A1 domain (aa 1204–1496) resulted in stepwise increased ristocetin-induced binding to human platelets (37); (iii) Ala mutations in the N-terminal flanking region of the A1 domain (aa 1260–1271) in full-length VWF resulted in an increased ristocetin-induced binding to human platelets (14); (iv) deletions in the aa 1222–1271 region in full-

length VWF in which an additional R1308A mutation was added resulted in an increased ristocetin-induced or even spontaneous binding to human platelets when compared with the R1308A VWF point mutant (38); (v) specific *O*-linked glycosylation in the aa 1248–1256 region negatively modulated the binding to human platelets as demonstrated using glycosylphosphatidylinositol COS-7 cell-anchored FLAG-tagged VWF A1 domains (39).

To further identify the exact residues within VWF important for the binding region of 1C1E7, we took advantage of the observation that 1C1E7 does not interact with porcine VWF. To confirm the putative role of the deviating residues in human *versus* pig VWF in maintaining the epitope of 1C1E7, a chimeric porcine/human VWF was constructed in which the aa 786–960 region of human VWF was exchanged by the corresponding porcine sequence. In the resulting recombinant protein, VWF(aa786–960)PIG, 22 of the possibly important residues were mutated. Compared with the published sequence, an extra mutation was inserted (P812L); however, in line with previous studies (40), this is probably a result of strain specificity, because sequencing of different cDNA clones resulted in the identification of the identical substitution. VWF(aa786–960)PIG, however, bound as good to 1C1E7 as did WT VWF, suggesting that the remaining aa 961–1035 region in VWF probably maintains the epitope of this moAb. Further mutagenesis of the rest of the differing residues identified Lys-968, located in the VWF D3 domain, as essential for the binding of moAb 1C1E7. As yet, this residue has not been linked with a functional deficiency of VWF. The ristocetin-induced interaction with rGPIbα of VWF(aa786–960)PIG containing an additional K968S mutation was slightly but significantly increased at submaximal doses of this modulator compared with WT VWF. Similar results were obtained in platelet agglutination studies (data not shown); in the presence of VWF(aa786–960)PIG and VWF(aa786–960)PIG-K968S, lower doses of ristocetin were needed to induce agglutination compared with WT VWF. These results would suggest that this residue and/or the surrounding region might be important for modulating the interaction of VWF with GPIbα. However, additional mutagenesis studies are needed to further confirm this.

VWF/D′D3 blocks both spontaneous and ristocetin-induced platelet agglutination in the presence of ΔD′D3. Similarly, VWF/D′D3 inhibited the spontaneous agglutination supported by ΔD′D3 (data not shown). This is in line with our hypothesis that in solution the D′D3 region interacts with structures in ΔD′D3 and that these intramolecular interactions in VWF shield the A1 domain from interacting with GPIbα.

It is known that immobilization of VWF is a prerequisite for platelet adhesion at high shear stress, probably due to conformational changes (41). However, the exact nature of these conformational changes has not been elucidated yet (42).

To further substantiate the idea that D′D3 would interact with A1 in VWF in solution and no longer when immobilized/sheared, we looked to whether moAbs against the respective domains would block each other's binding or not under those conditions when VWF was immobilized on a polystyrene surface, as it is known that this allows platelet recruitment (34). The anti-D′D3 moAb 418 cross-competed with the anti-A1 domain moAbs 701 and 724 when VWF was in solution, but not on immobilized VWF, indeed providing evidence for a changing distance between the domains upon immobilization. Previous studies suggested a structural change in the D′D3 region upon immobilization of VWF onto calf skin collagen, causing a reduced affinity for factor VIII (43). It could be that similar conformational changes in the D′D3 region are induced by immobilization of VWF on a polystyrene surface, leading to disruption of the structural proximity of this region with the A1 domain, thereby exposing the GPIbα binding site.

Finally, we also found a striking sequence similarity between the primary sequence of the complimentarity determining region 3 of the 1C1E7 heavy chain and the N-terminal flanking region of the VWF A1 domain (aa 1260–1271). This N-terminal flanking region is important in modulating the binding of the A1 domain with GPIbα as modifications or deletions in this region increase the affinity of VWF for GPIbα (14, 38), and in our view this might be the region within the A1 domain that interacts with the D′D3 region. 1C1E7 then would compete with this N-terminal flanking region disrupting this interaction. Because 1C1E7 interacts with K968 in the D3 domain, it is possible that the N-terminal flanking region interacts with this residue as well.

In conclusion, our results demonstrate an inhibitory role for the aa 764–1035 region in VWF for the GPIbα interaction. Based on these observations, the following hypothesis might be put forward. In native, resting conditions, the A1 domain and the D′D3 region are in close proximity, possibly through an interaction of the N-terminal flanking region of the A1 domain with the D3-domain, more precisely with the region of residue Lys-968. This interaction would limit the accessibility of the GPIbα binding site. When VWF is immobilized, this interaction is disrupted through conformational changes in VWF, possibly in the D′D3 region which allows recruitment of platelets through their GPIb-IX-V complex. Further studies are required to confirm this hypothesis.

REFERENCES

1. Ruggeri, Z. M. (2002) *Nat. Med.* **8,** 1227–1234
2. Vermylen, J., Donati, M. B., De Gaetano, G., and Verstraete, M. (1973) *Nature* **244,** 167–168
3. Vicente, V., Houghten, R. A., and Ruggeri, Z. M. (1990) *J. Biol. Chem.* **265,** 274–280
4. Read, M. S., Smith, S. V., Lamb, M. A., and Brinkhous, K. M. (1989) *Blood* **74,** 1031–1035
5. Siedlecki, C. A., Lestini, B. J., Kottke-Marchant, K. K., Eppell, S. J., Wilson, D. L., and Marchant, R. E. (1996) *Blood* **88,** 2939–2950
6. Lankhof, H., Wu, Y. P., Vink, T., Schiphorst, M. E., Zerwes, H. G., de Groot, P. G., and Sixma, J. J. (1995) *Blood* **86,** 1035–1042
7. Andrews, R. K., Gorman, J. J., Booth, W. J., Corino, G. L., Castaldi, P. A., and Berndt, M. C. (1989) *Biochemistry* **28,** 8326–8336
8. Gralnick, H. R., Williams, S., McKeown, L., Kramer, W., Krutzsch, H., Gorecki, M., Pinet, A., and Garfinkel, L. I. (1992) *Proc. Natl. Acad. Sci. U. S. A.* **89,** 7880–7884
9. Miura, S., Li, C. Q., Cao, Z., Wang, H., Wardell, M. R., and Sadler, J. E. (2000) *J. Biol. Chem.* **275,** 7539–7546
10. Huizinga, E. G., Tsuji, S., Romijn, R. A., Schiphorst, M. E., de Groot, P. G., Sixma, J. J., and Gros, P. (2002) *Science* **297,** 1176–1179
11. Dumas, J. J., Kumar, R., McDonagh, T., Sullivan, F., Stahl, M. L., Somers, W. S., and Mosyak, L. (2004) *J. Biol. Chem.* **279,** 23327–23334
12. Emsley, J., Cruz, M., Handin, R., and Liddington, R. (1998) *J. Biol. Chem.* **273,** 10396–10401
13. Meyer, D., Fressinaud, E., Hilbert, L., Ribba, A. S., Lavergne, J. M., and Mazurier, C. (2001) *Best. Pract. Res. Clin. Haematol.* **14,** 349–364
14. Matsushita, T., and Sadler, J. E. (1995) *J. Biol. Chem.* **270,** 13406–13414
15. Tornai, I., Arnout, J., Deckmyn, H., Peerlinck, K., and Vermylen, J. (1993) *J. Clin. Investig.* **91,** 273–282
16. Ulrichts, H., Harsfalvi, J., Bene, L., Matko, J., Vermylen, J., Ajzenberg, N., Baruch, D., Deckmyn, H., and Tornai, I. (2004) *J. Thromb. Haemost.* **2,** 1622–1628
17. Vanhoorelbeke, K., Depraetere, H., Romijn, R. A. P., Huizinga, E. G., De Maeyer, M., and Deckmyn, H. (2003) *J. Biol. Chem.* **278,** 37815–37821
18. Depraetere, H., Ajzenberg, N., Girma, J. P., Lacombe, C., Meyer, D., Deckmyn, H., and Baruch, D. (1998) *Blood* **91,** 3792–3799
19. Obert, B., Houllier, A., Meyer, D., and Girma, J. P. (1999) *Blood* **93,** 1959–1968
20. Pietu, G., Ribba, A. S., Meulien, P., and Meyer, D. (1989) *Biochem. Biophys. Res. Commun.* **163,** 618–626
21. Vanhoorelbeke, K., Cauwenberghs, N., Vauterin, S., Schlammadinger, A., Mazurier, C., and Deckmyn, H. (2000) *Thromb. Haemostasis* **83,** 107–113
22. Subramani, S., Mulligan, R., and Berg, P. (1981) *Mol. Cell. Biol.* **1,** 854–864
23. Lenting, P. J., Westein, E., Terraube, V., Ribba, A. S., Huizinga, E. G., Meyer, D., de

Groot, P. G., and Denis, C. V. (2004) *J. Biol. Chem.* **279,** 12102–12109

24. Staelens, S., Desmet, J., Ngo, T. H., Vauterin, S., Pareyn, I., Barbeaux, P., Van, R., I, Stassen, J. M., Deckmyn, H., and Vanhoorelbeke, K. (2005) *Mol. Immunol.,* in press

25. Sblattero, D., and Bradbury, A. (1998) *Immunotechnology* **3,** 271–278

26. Lilie, H., Schwarz, E., and Rudolph, R. (1998) *Curr. Opin. Biotechnol.* **9,** 497–501

27. Ulrichts, H., Vanhoorelbeke, K., Cauwenberghs, S., Vauterin, S., Kroll, H., Santoso, S., and Deckmyn, H. (2003) *Arterioscler. Thromb. Vasc. Biol.* **23,** 1302–1307

28. Fujimura, Y., Titani, K., Usami, Y., Suzuki, M., Oyama, R., Matsui, T., Fukui, H., Sugimoto, M., and Ruggeri, Z. M. (1991) *Biochemistry* **30,** 1957–1964

29. van der Plas, R. M., Gomes, L., Marquart, J. A., Vink, T., Meijers, J. C., de Groot, P. G., Sixma, J. J., and Huizinga, E. G. (2000) *Thromb. Haemostasis* **84,** 1005–1011

30. Sixma, J. J., Schiphorst, M. E., Verweij, C. L., and Pannekoek, H. (1991) *Eur. J. Biochem.* **196,** 369–375

31. Ruggeri, Z. M., and Zimmerman, T. S. (1981) *Blood* **57,** 1140–1143

32. Goudemand, J., Mazurier, C., Parquet-Gernez, A., and Goudemand, M. (1977) *Pathol. Biol.* (*Paris*) **25,** 241–243

33. Sugimoto, M., Ricca, G., Hrinda, M. E., Schreiber, A. B., Searfoss, G. H., Bottini, E., and Ruggeri, Z. M. (1991) *Biochemistry* **30,** 5202–5209

34. Ulrichts, H., Vanhoorelbeke, K., Girma, J. P., Lenting, P. J., Vauterin, S., and Deckmyn, H. (2005) *J. Thromb. Haemost.* **3,** 552–561

35. Dong, J. F., Berndt, M. C., Schade, A., McIntire, L. V., Andrews, R. K., and Lopez, J. A. (2001) *Blood* **97,** 162–168

36. Mohri, H., Fujimura, Y., Shima, M., Yoshioka, A., Houghten, R. A., Ruggeri, Z. M., and Zimmerman, T. S. (1988) *J. Biol. Chem.* **263,** 17901–17904

37. Sugimoto, M., Dent, J., McClintock, R., Ware, J., and Ruggeri, Z. M. (1993) *J. Biol. Chem.* **268,** 12185–12192

38. Nakayama, T., Matsushita, T., Dong, Z., Sadler, J. E., Jorieux, S., Mazurier, C., Meyer, D., Kojima, T., and Saito, H. (2002) *J. Biol. Chem.* **277,** 22063–22072

39. Schulte am Esch, J., Robson, S. C., Knoefel, W. T., Eisenberger, C. F., Peiper, M., and Rogiers, X. (2005) *Br. J. Haematol.* **128,** 82–90

40. Schulte am Esch, J., Cruz, M. A., Siegel, J. B., Anrather, J., and Robson, S. C. (1997) *Blood* **90,** 4425–4437

41. Savage, B., Almus-Jacobs, F., and Ruggeri, Z. M. (1998) *Cell* **94,** 657–666

42. Novak, L., Deckmyn, H., Damjanovich, S., and Harsfalvi, J. (2002) *Blood* **99,** 2070–2076

43. Bendetowicz, A. V., Wise, R. J., and Gilbert, G. E. (1999) *J. Biol. Chem.* **274,** 12300–12307